The Diurnal Cycle in the Tropics

GUI-YING YANG AND JULIA SLINGO

Centre for Global Atmospheric Modelling, Department of Meteorology, University of Reading, Reading, United Kingdom

(Manuscript received 6 March 2000, in final form 22 August 2000)

ABSTRACT

A global archive of high-resolution (3-hourly, 0.5° latitude–longitude grid) window (11–12 μm) brightness temperature (T_b) data from multiple satellites is being developed by the European Union Cloud Archive User Service (CLAUS) project. It has been used to construct a climatology of the diurnal cycle in convection, cloudiness, and surface temperature for all regions of the Tropics. An example of the application of the climatology to the evaluation of the climate version of the U.K. Met. Office Unified Model (UM), version HadAM3, is presented.

The characteristics of the diurnal cycle described by the CLAUS data agree with previous observational studies, demonstrating the universality of the characteristics of the diurnal cycle for land versus ocean, clear sky versus convective regimes. It is shown that oceanic deep convection tends to reach its maximum in the early morning. Continental convection generally peaks in the evening, although there are interesting regional variations, indicative of the effects of complex land–sea and mountain–valley breezes, as well as the life cycle of mesoscale convective systems. A striking result from the analysis of the CLAUS data has been the extent to which the strong diurnal signal over land is spread out over the adjacent oceans, probably through gravity waves of varying depths. These coherent signals can be seen for several hundred kilometers and in some instances, such as over the Bay of Bengal, can lead to substantial diurnal variations in convection and precipitation.

The example of the use of the CLAUS data in the evaluation of the Met. Office UM has demonstrated that the model has considerable difficulty in capturing the observed phase of the diurnal cycle in convection, which suggests some fundamental difficulties in the model's physical parameterizations. Analysis of the diurnal cycle represents a powerful tool for identifying and correcting model deficiencies.

1. Introduction

The most fundamental modes of variability of the global climate system are the diurnal and seasonal cycles, which are associated with large and well-defined variations in the solar forcing. As basic, forced modes of the climate system, the ability of general circulation models to represent these cycles should be a key test of the correctness of any model. On both diurnal and seasonal timescales, the proper representation of the interaction between the various elements of the atmosphere–land–ocean–cryosphere system is crucial for achieving the correct amplitude and phase of these forced modes. In particular, an accurate representation of the diurnal cycle over land and ocean provides a key test of many aspects of the physical parametrizations in a climate model, from radiative transfer and surface exchanges through to boundary layer, convective, and cloud processes. It could be argued, therefore, that the simulation of the amplitude and phase of the diurnal cycle provides an ideal test bed for model parametrizations and for the representation of the interactions between the surface, the boundary layer, and the free atmosphere.

The diurnal cycle in tropical cloudiness and precipitation has been extensively studied for several decades, but because of the scarcity of observational data, especially over the tropical oceans, these studies have used different data sources and have mostly been confined to limited regions. The earlier studies primarily used surface observations (e.g., Gray and Jacobson 1977; McGarry and Reed 1978; Albright et al. 1981), while later studies used various forms of satellite or radar-derived cloudiness and precipitation (e.g., Albright et al. 1985; Hendon and Woodberry 1993; Chang et al. 1995; Chen and Houze 1997; Sui et al. 1997; Garreaud and Wallace 1997). Most of these studies showed that the convective or precipitation maximum tended to occur in the early morning over the open oceans and in the late afternoon/early evening over land. However, some studies also showed an afternoon maximum in precipitation and cloudiness over the oceans (e.g., McGarry and Reed 1978; Augustine 1984; Shin et al. 1990). Janowiak et al. (1994) provided an extensive

Corresponding author address: Prof. Julia Slingo, CGAM, Department of Meteorology, University of Reading, Earley Gate, Whiteknights, Reading RG6 6BB, United Kingdom.
E-mail: j.m.slingo@reading.ac.uk

analysis of the diurnal cycle of cold clouds in the global tropics based on 3-hourly geostationary satellite data that had been averaged on to a 2.5° latitude–longitude grid. Their results confirmed the existence of an early morning maximum in the extent of the coldest cloud tops (temperatures $<$230 K) but also demonstrated that warmer clouds, typical of midlevel convection, were most prevalent in the afternoon.

Nevertheless, despite these studies, no climatology exists of all aspects of the diurnal cycle in tropical convection, cloudiness, and surface temperature that is representative for all regions of the Tropics and for all seasons, and that would be suitable, therefore, for climate model evaluation. Recent advances in the availability of global, and high spatial and temporal resolution satellite data have made it feasible to perform a comprehensive analysis of the diurnal cycle in cloudiness and surface temperature. Following the pioneering work of Salby et al. (1991), who created and demonstrated the utility of a global cloud imagery dataset based on multiple satellites, the European Union funded a project entitled Cloud Archive User Service (CLAUS), to construct an archive of global window brightness temperature (T_b) for the period 1983–present. The archive is based on the International Satellite Cloud Climatology Project (ISCCP) level B3 data (Rossow et al. 1997; Brest et al. 1997), which are then synthesised to provide a global dataset on a regular 0.5° latitude–longitude grid at 3-hourly intervals, the temporal sampling being sufficient to enable diagnosis of diurnal variability.

In this study, the CLAUS data are used to investigate the diurnal variation of tropical convection (and by implication precipitation), cloudiness, and surface temperature, and to provide a climatology of the amplitude and phase of the diurnal cycle for all regions of the Tropics (30°N–30°S). As an example of the application of the results to model evaluation, a diagnosis of the diurnal cycle in the Met. Office Unified Model has been performed and the results will be described briefly. The development of the CLAUS archive is described in section 2 and the methodology used to analyse the diurnal cycle will be given in section 3. Section 4 will present the main results of the analysis of the observed diurnal cycle, while an example of its application to model evaluation is given in section 5. Conclusions and discussion will be given in section 6.

2. Description of the CLAUS dataset

The aim of the CLAUS project is to create a global, long-term archive of window (11–12 μm) brightness temperature using the ISCCP intermediate level (B3) products (reduced resolution radiance data) from 1983 onward. The ISCCP data come from a variety of geostationary and polar orbiting satellites. These data are then resampled onto a global grid at a resolution of 0.5° latitude–longitude every 3 h beginning at 0000 UTC.

As part of the CLAUS project, a series of algorithms has been developed to minimize the effects of missing data and the varying geometries of the satellite sampling and viewing characteristics.[1] Although the approach used is similar to that of Salby et al. (1991), an improved algorithm for synthesizing the data from the various satellites has been developed and is described in detail in Hodges et al. (2000). This algorithm uses the window brightness temperatures from the multiple satellites, both geostationary and polar orbiting, which have already been navigated and normalized to the measurements from the National Oceanic and Atmospheric Administration's Advanced Very High Resolution Radiometer. The gridding involves a hierarchical scheme based on spherical kernel estimators. The geostationary data are corrected for limb effects using a simple empirical correction to the radiances. The polar orbiter data are windowed on the target time with temporal weighting to account for the nonlocal temporal nature of the data. To account for incomplete satellite coverage and for missing data, a combination of spatial and temporal interpolation has been applied to obtain continuity over space and time whenever possible. Large regions of missing data are interpolated from adjacent processed images using a form of motion compensated interpolation (Hodges et al. 2000).

As well as the brightness temperature data, quality control data are also generated to indicate (i) the degree of confidence of the interpolation at the pixel level, and (ii) the primary satellite being used in the generation of that data pixel. Most of the Tropics is well sampled by geostationary satellites except for the Indian Ocean where data from the Indian satellite were not made available to ISCCP. For a narrow swath centered on 70°E, data from polar orbiting satellites have been used instead. Due to the twice-daily crossing of these satellites, a strong semidiurnal harmonic is evident in the CLAUS data, which is an artifact of the sampling.

It is important to note here that the packing density of the ISCCP B3 data was relatively coarse, so that the precision of the gridded window brightness temperature in the CLAUS dataset is only of the order of 0.7 K. This is adequate for diagnosing the diurnal cycle in cumulus convection and land surface temperature, but may not be sufficient to delineate the subtle diurnal variations in sea surface temperatures (SSTs) and stratocumulus decks.

CLAUS data for four winters (Dec–Feb 1984/85, 1986/87, 1987/88, and 1991/92) and four summers (Jun–Aug 1985, 1986, 1987, and 1992) are currently available and have been used in this study. All results are based on an average over the four winters and four summers, respectively. There is considerable consistency between the characteristics of the diurnal cycle from

[1] See the CLAUS Web site at http://www.nerc-essc.ac.uk/CLAUS.

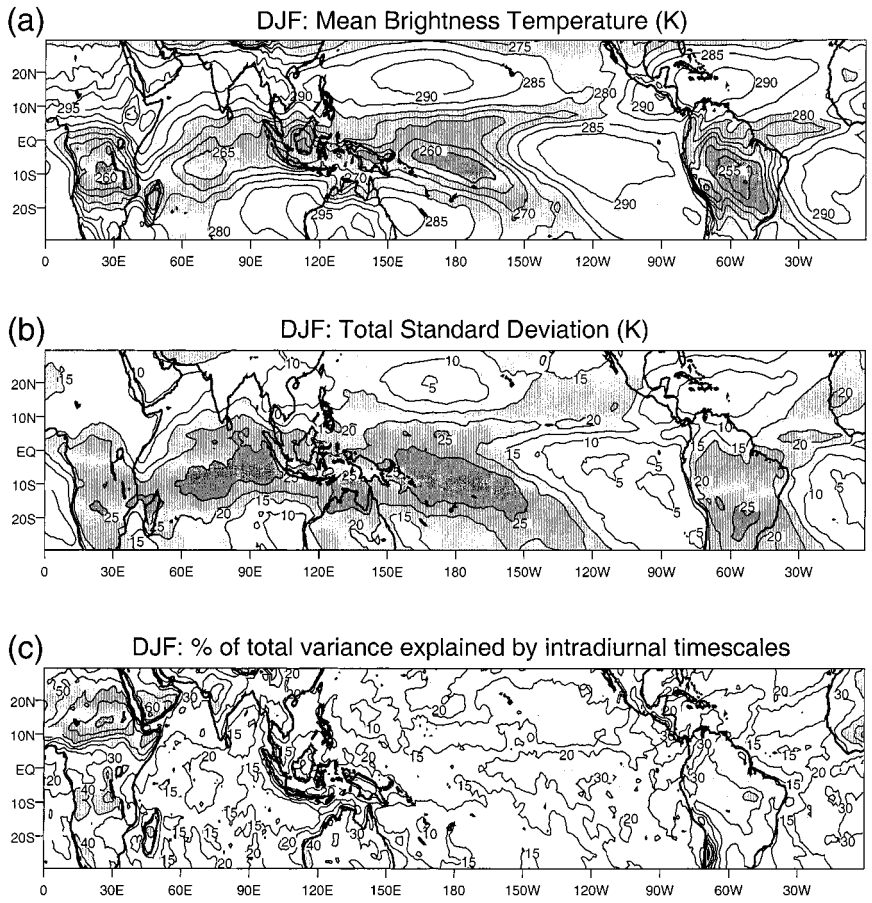

FIG. 1. Seasonal mean brightness temperature (K), total standard deviation (K), and percentage of total variance explained by intradiurnal (<1 day) timescales for (a)–(c) DJF and (d)–(f) JJA.

year to year, which suggests that 4 yr of data are sufficient to provide a useful climatology.

Figure 1 shows the seasonal mean brightness temperature for northern winter and summer, as well as the total standard deviation of the 3-hourly samples and the percentage of the total variance that is associated with intradiurnal (less than or equal to 1 day) timescales. The intradiurnal variance was computed by performing a spectral analysis of the brightness temperature time series at each grid point and then averaging the power for timescales less than or equal to 1 day. To perform this calculation accurately, it requires a complete time series at each grid point; grid points where this is not the case are therefore treated as missing data in Fig. 1.[2]

As expected, the seasonal mean brightness temperature distribution (Figs. 1a and 1d) follows the climatological distributions of outgoing longwave radiation (OLR) derived from broadband satellite measurements (e.g., Harrison et al. 1990) and also those of precipitation (e.g., Xie and Arkin 1996), with the coldest temperatures coincident with the minima in OLR and maxima in precipitation. The change in the mean brightness temperature field between December–January–February (DJF) and June–July–August (JJA) shows the seasonal transition of the intertropical convergence zone (ITCZ) and the movement of the major areas of convection associated with summertime continental convection and monsoons. In both seasons, the highest brightness temperatures tend to occur during summer over the desert areas of Australia and North Africa. High temperatures are also seen in the subsiding, dry, and predominantly cloud-free regions of the subtropical anticyclones.

Comparison of the total standard deviation of the brightness temperature (Figs. 1b and 1e) with the seasonal mean field shows that most of the convective regions, defined by low brightness temperatures, are coincident with regions of large standard deviation. This is in agreement with other observational and modeling studies (e.g., Salby et al. 1991; Slingo et al. 1992). Also it can be seen that for most of the nonconvective regions,

[2] The percentage variance explained by intradiurnal timescales was only computed for the three summers of 1986, 1987, and 1992 due to large areas of missing data during the summer of 1985. The winter datasets were all complete.

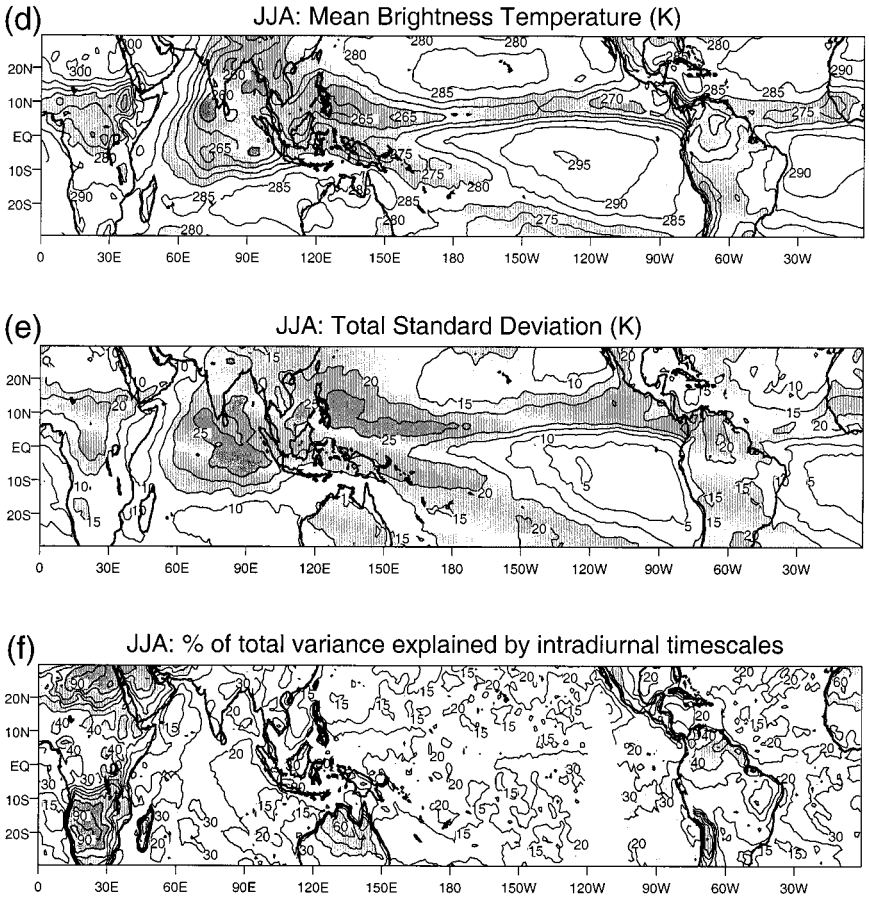

FIG. 1. (*Continued*)

such as the subtropical anticyclones, the standard deviation is small, the exceptions being the clear sky land regions, where the standard deviation is almost entirely related to intradiurnal timescales (Figs. 1c and 1f). Over the deep convective regions of the tropical oceans, intradiurnal timescales only account for between 15% and 20% of the total variability. As shown by several authors (e.g., Salby et al. 1991; Slingo et al. 1994) most of the variability in tropical oceanic convection is associated with synoptic systems (e.g., easterly waves) and intraseasonal phenomena (e.g., Madden–Julian oscillation). For land-based tropical convection, the intradiurnal timescales account for much more of the total variance, typically between 30% and 40%.

The results shown in Fig. 1 demonstrate that the CLAUS dataset provides a good climatology of tropical brightness temperature and therefore, by inference, convective activity and land surface temperatures. Through its high temporal sampling and global coverage, it also provides a good measure of tropical variability, in particular the degree to which that variability is associated with intradiurnal timescales. In the following section the methodology used to analyze the coherent diurnal cycle will be described.

3. Methodology for analyzing the diurnal cycle

Time series analysis and evolutionary histograms will be used to study the coherent diurnal cycle in tropical convection and land surface temperature. By computing the long-term (seasonal) mean for each of the eight times of the day (3-hourly intervals), the coherent diurnal variation, which is directly linked to the response of the surface–atmosphere system to the diurnal cycle in the solar radiation, can be obtained. The amplitude and phase of the diurnal and semidiurnal harmonics can then be calculated using Fourier analysis. The phase of the diurnal harmonic indicates the local time of the maximum in the variable considered. Calculation of the semidiurnal and 8-h harmonics showed that the amplitudes of these harmonics are much smaller, generally about 40% and 15% of that for the diurnal harmonic.

The evolutionary histogram approach, which has been used in several studies for analyzing the diurnal cycle (e.g., Morcrette 1991), will be used to show the composite diurnal evolution of convection and land surface temperature over various selected, nearly homogeneous, regions. In an evolution histogram of brightness temperature (T_b), the number of pixels (grid points) within

each T_b interval is plotted as a function of time of day. In general, high values of T_b correspond to radiation emitted from at or near the surface, and lower values to radiation emitted from clouds. This technique provides a clear overview of the evolution of surface temperature and convection with time of day. In this study, the evolution histograms are constructed by binning the 3-hourly T_b data into 4-K bins. The diurnal variation in the histogram of T_b is identified more clearly by computing the percentage anomaly at each 3-h interval against the daily mean histogram of T_b.

Currently, models do not diagnose a window brightness temperature comparable to that observed by satellites, although algorithms are being developed and implemented. Therefore, for the application of the CLAUS data to model evaluation, it has been necessary to transform the model output and the CLAUS data to common variables. First, the model's OLR has been converted to an equivalent brightness temperature using the relationship between the observed window brightness temperature (T_b) and the flux equivalent brightness temperature (T_f), as proposed by Ohring and Gruber (1984):

$$T_f = T_b(a + bT_b), \tag{1}$$

where $a = 1.228$ and $b = -1.106 \times 10^{-3}$ K^{-1}. Then T_f is related to OLR by

$$\text{OLR} = \sigma T_f^4, \tag{2}$$

where σ is the Planck constant. Second, the CLAUS data have been converted to equivalent precipitation on the basis that the coverage of cold clouds (with brightness temperature or equivalent blackbody temperature less than some threshold) is correlated with accumulations of precipitation during some period (e.g., Richards and Arkin 1981; Hendon and Woodberry 1993; Goodman et al. 1993). In this study, a threshold technique for estimating tropical deep convective precipitation, developed by Hendon and Woodberry (1993) and used for studying the diurnal cycle in tropical convection, has been applied to the CLAUS data. Known as the deep convective activity (DCA) index, it relates brightness temperature to an equivalent precipitation rate:

$$\text{DCA} = \begin{cases} a(230 - T_b) & \text{for } T_b < 230 \text{ K} \\ 0 & \text{otherwise,} \end{cases} \tag{3}$$

where $a = 0.29$ mm h^{-1} K^{-1}, and the choice of the 230-K threshold is based on the work of Fu et al. (1990). The seasonal mean precipitation rate produced by applying Eq. (3) to the CLAUS data compares well with other precipitation climatologies (e.g., Xie and Arkin 1996). The advantage of converting the observed brightness temperature to an equivalent precipitation rate is that it provides a different view of the diurnal cycle; it delineates the diurnal cycle in deep convection (i.e., cold cloud tops) from that in land surface temperatures. As already discussed in section 2, the transient characteristics of convective and nonconvective regimes are different, with the variability over clear sky land areas being dominated by intradiurnal timescales (Fig. 1).

4. Observed diurnal cycle in brightness temperature and derived precipitation

a. Amplitude and phase of the diurnal cycle

Figure 2 shows the amplitude of the diurnal (24 h) harmonic in brightness temperature (T_b) and estimated precipitation (DCA algorithm) for northern winter (DJF) and northern summer (JJA), respectively.[3] For both seasons, the largest amplitude of T_b occurs over land clear sky regions, as a result of the large response of the surface temperature to daytime solar heating. The maxima in the amplitude of the diurnal cycle in T_b occur over the Atacama and Namib Deserts in DJF and over Saudi Arabia and the Sahara and Kalahari Deserts in JJA. The convective regions over land (e.g., South America in DJF, Indian subcontinent in JJA, Indonesian Islands) also show large amplitudes for T_b, consistent with the forcing of convection by the diurnal cycle in land surface heating. This is particularly pronounced over northeast India during the summer monsoon season and demonstrates the importance of the diurnal cycle in modulating monsoon rainfall. An interesting feature of Fig. 2 is the spreading of the diurnal amplitude from land convective regions out over the adjacent oceans, suggestive of complex land–sea-breeze effects. This is especially marked around the Indonesian Islands in DJF, and over the northern Bay of Bengal and along the Central American and Mexican coasts in JJA.

Over the majority of the tropical oceans, the diurnal cycle is much more subtle and is best captured by the estimated precipitation field, which focuses on the variations in the cold cloud amounts. The results shown in Figs. 2c and 2d demonstrate that there is a small but significant diurnal variation in oceanic precipitation of the order of 3–6 mm day^{-1} along the ITCZ and South Pacific convergence zone (SPCZ) in both seasons. The amplitude of the diurnal cycle inferred from the CLAUS data is similar to that suggested by Janowiak et al. (1994) and Chang et al. (1995) based on Special Sensor Microwave/Imager data.

The phase of the diurnal harmonic of brightness temperature and estimated precipitation for DJF and JJA is given in Fig. 3 in terms of the *local time* of the maximum. Over clear sky land regions, such as the Sahara, the maximum in T_b occurs consistently about 1–2 h after the peak in the solar heating, indicative of a slight lag in the land surface heating due to the thermal inertia of the soil. In comparison, over oceanic clear sky/nonconvective regions, such as the subtropical anticyclones and

[3] The diagnosis was also completed for the transition seasons, March–May and September–November. The results were similar and will not be shown here.

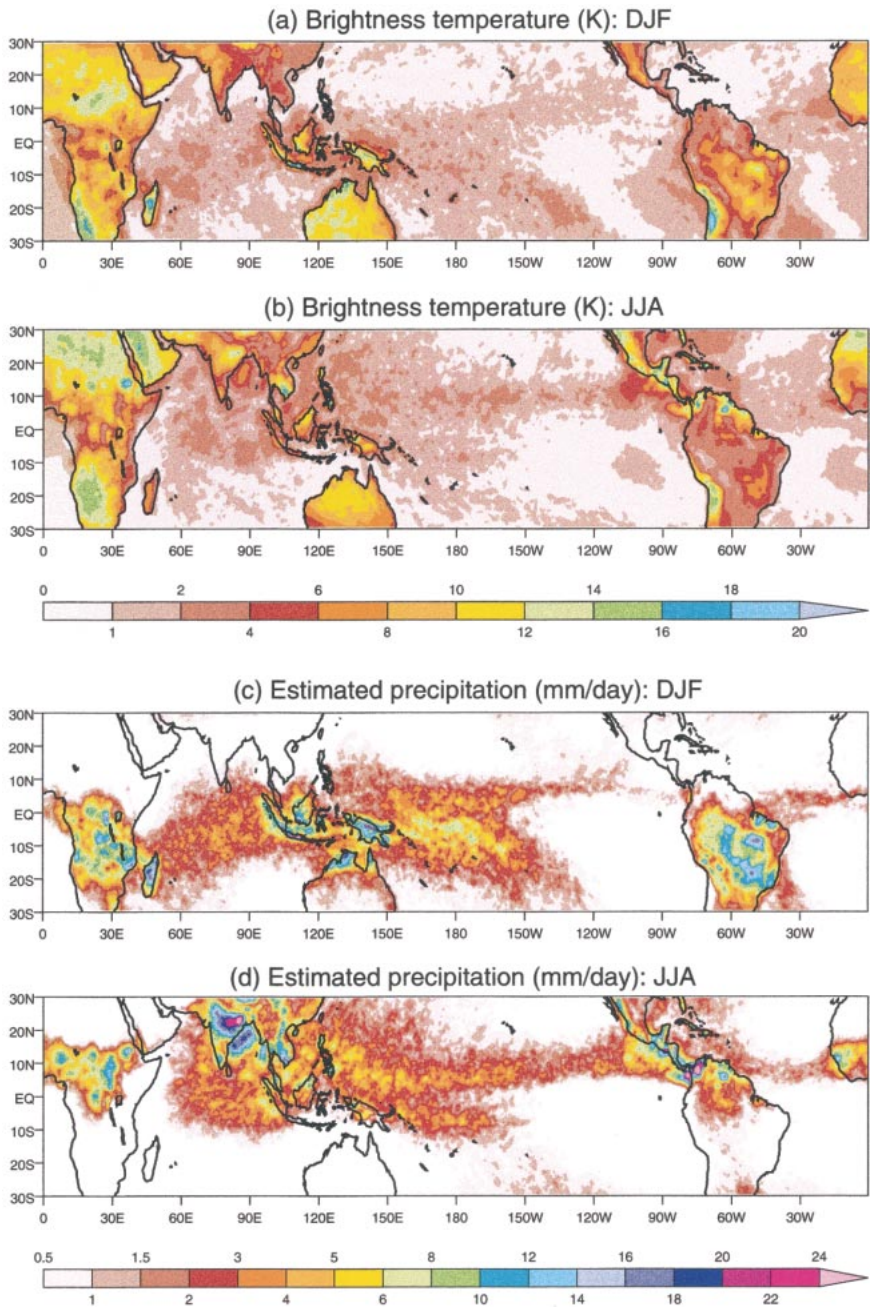

FIG. 2. Seasonal mean amplitude of the diurnal harmonic in brightness temperature (K) and estimated precipitation (mm day^{-1}) for DJF and JJA.

the stratocumulus regions off the western seaboards, the maximum in T_b occurs in the mid- to late afternoon. However, this result may not be very robust since the amplitude of the diurnal cycle is small and the precision of the raw T_b data is rather poor, due to the packing density of the ISCCP B3 data (see section 2). Nevertheless, the phase results are entirely consistent with other observations of the diurnal cycle in marine stratocumulus (e.g., Hignett 1991; Bergman and Salby 1996), which have shown a minimum in cloud optical depth/amount in the late afternoon. This has been explained by, first, the decoupling of the surface and planetary boundary layers during the day, which leads to a reduction in the surface moisture supply to the cloud layer, and second, by the shortwave radiative warming of the cloud layer itself (e.g., Smith and Kao 1996).

The phase of the diurnal harmonic in the estimated precipitation (Figs. 3c and 3d) emphasizes the timing of the maximum in deep convection. The continental areas show that the maximum in deep convection/pre-

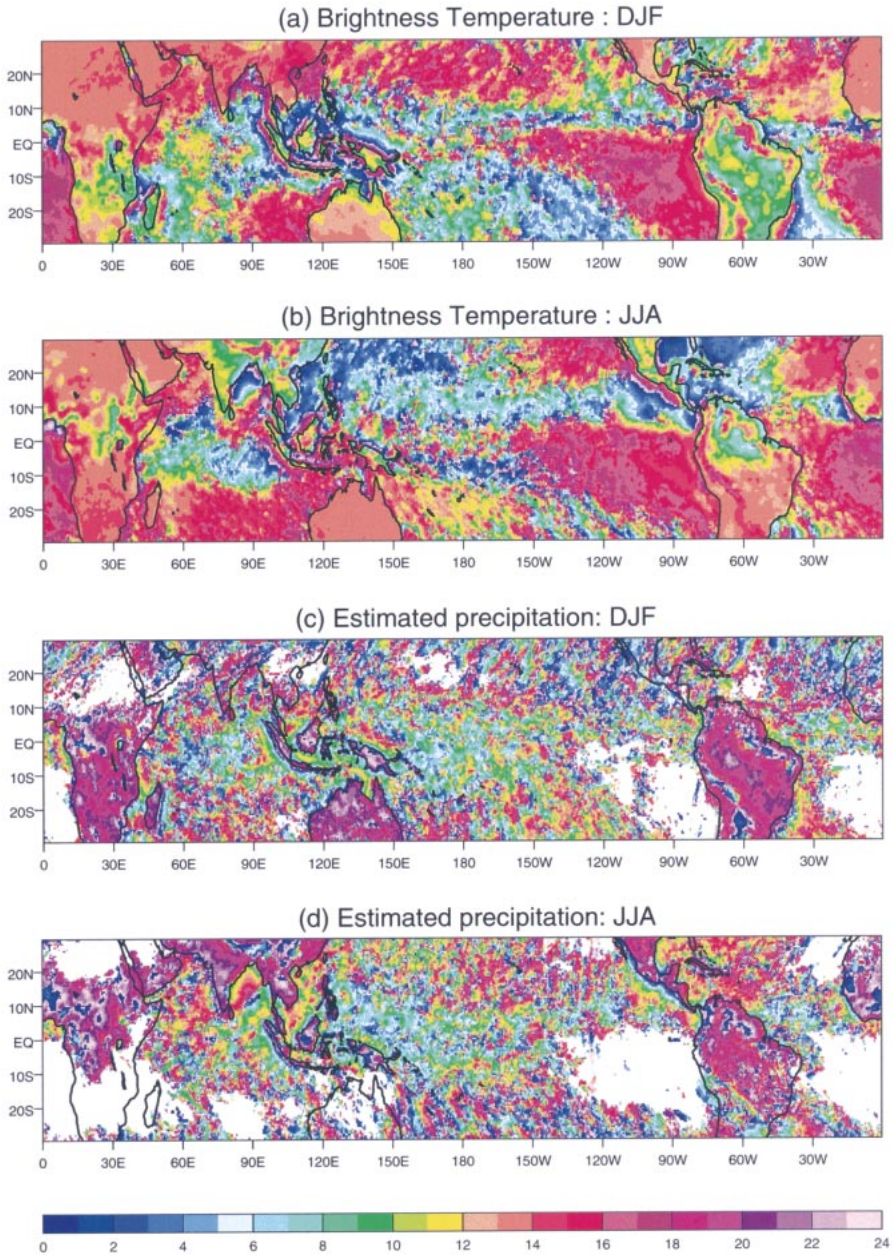

FIG. 3. Seasonal mean phase of the diurnal harmonic of brightness temperature and estimated precipitation for DJF and JJA. Local time of the maximum is given.

cipitation tends to occur in the late afternoon and evening, between 1700 and midnight local time. However, there are some interesting regional variations (e.g., central Africa, 0°–20°N, in JJA) which suggest that orography may play an important part in modulating the phase of the diurnal cycle. Over Africa, mesoscale convective systems (MCSs; e.g., squall lines) are often triggered by orography and elevated daytime heating (e.g., Rowell and Milford 1993; Hodges and Thorncroft 1997). In Fig. 2d, there is a good correspondence between the maxima in the amplitude of the diurnal harmonic and the elevated terrain of the Ethiopian Highlands, the Cameroon Highlands, Jos, Air, and the Guinea Highlands. Hodges and Thorncroft (1997) show that these MCSs are typically initiated around 1700 and 1800 local time, and that their lifetime varies from a few hours to more than a day. Their propagation, usually westward away from their source regions, means that the phase of the diurnal harmonic may portray a later and later time as the MCS moves farther and farther away from its source region. McGarry and Reed (1978) offer this explanation for the near-midnight maximum in precip-

itation that was observed over West Africa during the Global Atmospheric Research Programme (GARP) Atlantic Tropical Experiment (GATE). The results from this analysis of the CLAUS data, combined with the initiation and lifetime of MCSs given by Hodges and Thorncroft (1997), appear to support this explanation.

Similar interactions between orography and diurnal heating are also suggested by the rather complex variations in the phase of the diurnal harmonic over South America, for example along the Andes in DJF. Kousky (1980) describes a detailed analysis of the diurnal rainfall variations over northeast Brazil, which suggests a complex arrangement of land–sea and mountain–valley breezes. The CLAUS results shown in Fig. 3 provide further evidence that the phase of the diurnal cycle in precipitation/convection is much more variable than the late afternoon/evening maximum suggested by, for example, Wallace (1975), who related it to daytime boundary layer heating.

Nevertheless, over quite extensive areas of South Africa, and South and Central America, where orographic influences are small and convection is less well organized than over central and West Africa, there is a strong tendency for the maximum in precipitation/convection to occur between 1700 and 2000 local time. This timing is consistent with the results of Gray and Jacobson (1977) who analyzed the incidence of moderate to heavy precipitation using the present weather codes reported by a large number of land surface stations from South America and Africa.

Over the oceans, the phase of the diurnal cycle is very variable, although for regions of deep convection (characterized by low T_b in Fig. 1), away from any influence of land-forced diurnal variations, the precipitation tends to peak in the early morning, around 0600 local time, as noted by Janowiak et al. (1994) using satellite measurements of cold clouds. However, this result needs to be treated with caution since there are potential inconsistencies between the actual timing of the precipitation maximum and that inferred from the brightness temperature using Eq. (3). Janowiak et al. (1994) present results from in situ measurements of rainfall during Tropical Ocean Global Atmosphere Coupled Ocean–Atmosphere Response Experiment (TOGA COARE), which show that, in disturbed conditions, the maximum precipitation generally occurred near 0300 local time, some 3 h earlier than the maximum extent of cold clouds ($T_b < 230$ K). Gray and Jacobson (1977) also report oceanic precipitation maxima prior to 0600 local time, nearer 0400 local time. Similarly, McGarry and Reed (1978) noted that, over West Africa, the rainfall maxima preceded the convective cloud maxima by up to 2 h, which they associated with the spreading out of the convective cloud tops after the peak in precipitation. This apparent discrepancy between the actual and inferred timing of the precipitation maximum is important when satellite data are used to evaluate model behavior.

The rather variable phase results over the oceanic convective regions are perhaps not surprising bearing in mind the complex diurnal cycles in tropical convection described by Sui et al. (1997) based on TOGA COARE observations. They noted that only the deep, organized convection tended to show an early morning maximum whereas submesoscale convection, typical of suppressed conditions, tended to show a late afternoon maximum, much more similar to land-based convection. They relate this to the diurnal cycle in the ocean skin temperature, which can be pronounced in light wind conditions (e.g., Weller and Anderson 1996). Similarly, Janowiak et al. (1994) noted that, whereas the coldest clouds ($T_b < 230$ K) tended to show an early morning maximum, warmer clouds ($T_b > 235$ K) were most prevalent in the afternoon.

The CLAUS results also suggest that there is a notable difference in the phasing of the diurnal cycle between the Atlantic sector and the Pacific and Indian Oceans. In JJA (Figs. 3b and 3d), there is a uniform signal over the Caribbean, Gulf of Mexico, and the northwest Atlantic of a maximum in T_b near midnight. The most likely explanation is that these regions are dominated by warmer clouds whose behavior is more similar to the submesoscale cumulus congestus extensively observed in TOGA COARE (Johnson et al. 1999), and whose diurnal variation is more typical of land-based convection with maximum cloudiness in the late afternoon (e.g., Sui et al. 1997).

A notable feature of the GATE results was the tendency for the precipitation over the ship array (5°–12°N, 20°–27°W) to occur in the afternoon (McGarry and Reed 1978; Albright et al. 1981), at odds with the oceanic early morning maximum suggested by Gray and Jacobson (1977). The CLAUS results for JJA show a similar pattern, with an afternoon maximum being more likely east of 30°W (Fig. 3d).

The spreading of the diurnal cycle from coastal regions out over the surrounding oceans has already been noted in Fig. 2. This effect is particularly striking in the phase of the diurnal harmonic. Closer examination of Fig. 3 shows coherent diurnal variations propagating away from the coasts of the Indonesian islands in DJF, down the Bay of Bengal in JJA, southwestward away from the Mexican coast in JJA, and off the West African coast in JJA. In many cases these coherent diurnal variations spread out for many hundreds of kilometers. It is clear, particularly from the results for T_b (Fig. 3b), that the phase of the diurnal cycle over the GATE ship array, noted above, may well be associated with the remote effects of the diurnal cycle over the adjacent West African landmass.

From the timing of the lines of constant phase seen in Fig. 3, it is possible to estimate the propagation speed of the signal as it moves away from the coast. Figure 4 shows a close-up view of the phase of the maximum brightness temperature over the Bay of Bengal in JJA. Starting from the northeast coast of India, lines of con-

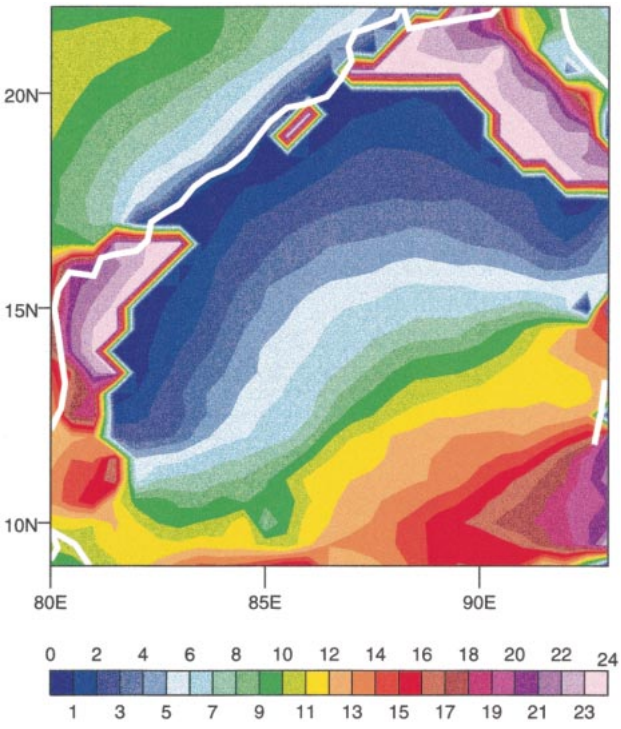

FIG. 4. Phase of the diurnal harmonic of brightness temperature over the Bay of Bengal in JJA in terms of the local time of the maximum. The coastline is marked in white.

stant phase spread out southeastward across the Bay of Bengal. The inferred propagation speed is between 15 and 20 m s^{-1}, in line with those of coherent disturbances that were observed propagating rapidly southward over the Bay of Bengal during the recent Joint Air–Sea Monsoon Interaction Experiment (JASMINE; P. Webster 2000, personal communication). As shown in Fig. 2d, these propagating disturbances generate significant diurnal variations in precipitation over the Bay of Bengal, suggesting that these waves have a fairly deep structure. In fact, the inferred propagation speed is consistent with that expected for a diurnally generated gravity wave whose equivalent depth is 40 m and whose spatial scale is wavenumber 20. The fact that the lines of constant phase tend to run parallel to the coast in Fig. 4 suggests that this coherent diurnal variation is probably triggered by the diurnal cycle over the land. Figure 2d has already shown a maximum in the diurnal amplitude of precipitation over northeast India; its spatial scale is about 10°, consistent with the inferred gravity wave spatial scale noted above.

The lines of constant phase around the islands of Indonesia in DJF (Figs. 3a and 3c) suggest a complex system of diurnally varying convection over the Maritime Continent. Here the inferred propagation speed away from the islands is slower than over the Bay of Bengal case, being typically nearer 10 m s^{-1}. Again the signal is evident for many hundreds of kilometers, for example, northeastward of New Guinea in DJF (Figs. 3a and 3c). Similarly the lines of constant phase spreading away from the Mexican coast in JJA also suggest a slower propagation speed than seen in Fig. 4 for the Bay of Bengal. If the signal is associated with a gravity wave, then the slower speed is probably indicative of a shallower wave, more typical of a sea–land-breeze effect. This is consistent with the amplitude of the signal in precipitation/deep convection being weaker for the Indonesian islands and Mexican coast than for the Bay of Bengal (Fig. 2).

During the Winter Monsoon Experiment, pronounced diurnal variations around Borneo were observed (Houze et al. 1981; Williams and Houze 1987), similar to those described here. A morning maximum in convection was noted off the northwest coast of Borneo, which Johnson and Kriete (1982) interpreted as an interaction between the northeast monsoon flow and the nighttime land breeze off Borneo. They noted that the structure of the disturbance was very similar to a squall line, much as was observed over the Bay of Bengal during JASMINE. In addition, Mapes and Houze (1993) have commented on the afternoon maximum in convection over the islands of the Maritime Continent with a related, but lesser, peak over the surrounding seas during the night and morning. The results from this analysis of the CLAUS data show that these coherent diurnal variations around the islands are widespread and ubiquitous, indicating that diurnally forced sea–land breezes and their influence on organized convection may be an important component of the hydrological cycle and energy budget of the Maritime Continent.

b. Evolution histograms for selected regions with different characteristics

To investigate the diurnal cycle in more detail for particular regions with different characteristics, evolution histograms have been constructed. Based on the seasonal mean field T_b and its variability (Fig. 1), various regions have been selected whose characteristics are nearly homogeneous and that represent different climatic regimes (e.g., deep oceanic convection, clear sky land). Figures 5 and 6 show the evolution histograms of T_b over three[4] particular regions for DJF and JJA, respectively. These have been constructed as described in section 3; since the areas chosen cover a minimum of 1200 data points, which are sampled over 3 months and over the 4 yr available, the histograms are well sampled. These results complement those shown earlier for the diurnal harmonic and demonstrate how well the diurnal cycle can be represented by a harmonic analysis. They also show the more general characteristics of the diurnal cycle for a particular climatic regime and are therefore particularly useful for model evaluation.

[4] Several others were also studied but will not be shown here since the results are very similar.

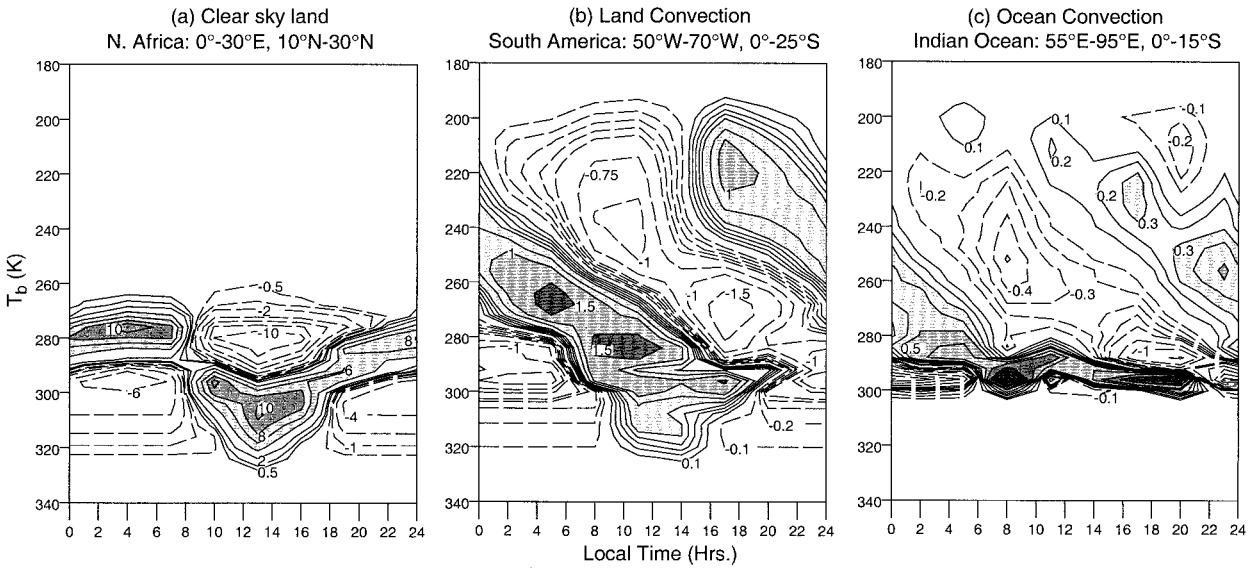

FIG. 5. Seasonal mean evolution histograms of the diurnal variation in brightness temperature for DJF. The contours represent percentage departures from the daily mean histogram of brightness temperature.

For clear sky land conditions (Figs. 5a and 6a), the evolution histograms confirm that the maximum brightness temperature occurs just after noon, consistent with the phase of the diurnal harmonic in T_b seen in Fig. 3. However, the evolution histograms suggest that the minimum T_b occurs between 0400 and 0600 local time, just before dawn, with a diurnal range in T_b of typically around 30 K. This timing of the maximum T_b and the evolution of T_b, as shown in Figs. 5a and 6a, are in agreement with the detailed study of the diurnal cycle over Kansas, observed during the First International Satellite Land Surface Climatology Project (ISLSCP) Field Experiment and described by Betts and Ball (1995). They report a minimum 2-m temperature just before sunrise, between 0500 and 0600 local time, and a maximum temperature 1–2 h after local noon.

Comparison of the land convection with the land clear sky examples (Figs. 5a,b and 6a,b) demonstrates, as expected, the importance of the warming of the land surface in triggering convection. Over both South America in DJF and central Africa in JJA, deep convection develops in the late afternoon and reaches a maximum in the evening. Thereafter the histograms suggest that the clouds decay during the early morning hours, dissipating at or just before sunrise. This allows the land surface temperatures to increase in the morning hours,

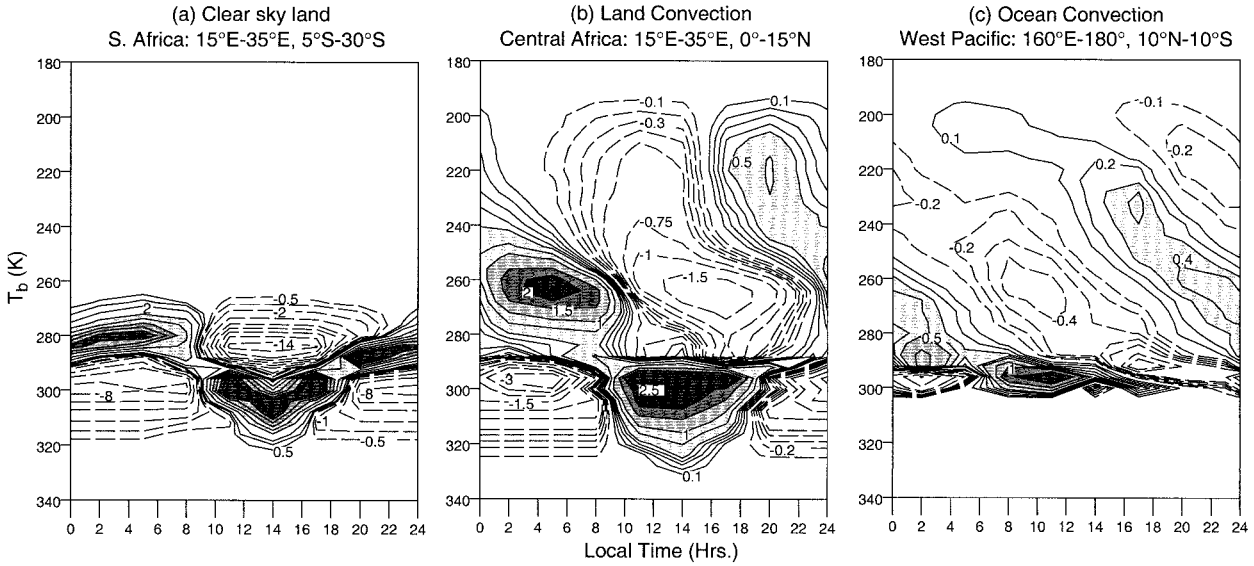

FIG. 6. As in Fig. 5 but for JJA.

and the whole cycle repeats itself. Again, these results are broadly consistent with the phases of the diurnal harmonics of T_b and estimated precipitation shown in Fig. 3.

Even though the amplitude of the diurnal harmonic in T_b is small over the tropical oceans (Fig. 2), the size of the sample used to construct the evolution histograms has enabled a clear signal of the diurnal cycle in deep convection to be identified (Figs. 5c and 6c). As suggested by the phase of the diurnal harmonic in estimated precipitation (Fig. 3), which focuses on cold clouds, the evolution histograms confirm that deep convection tends to peak during the early morning. The coldest clouds, with T_b near 200 K, always occur preferentially between 0200 and 0600 local time. Where the convection tends to be slightly less deep (T_b between 200 and 220 K) the maximum occurrence of cold clouds is slightly later, between 0600 and 1000 local time. This is typical of the Atlantic ITCZ in JJA and the SPCZ in DJF.

The histograms also show that the very coldest clouds occur over the west Pacific in DJF, consistent with the maximum height and coldness of the tropopause, as diagnosed by Highwood and Hoskins (1998). Conversely, convection in the Atlantic ITCZ is never as deep as over the west Pacific; the coldest T_b over the Atlantic is typically 10–20 K warmer than over the west Pacific. Again, this result is consistent with the lower/warmer tropopause over the Atlantic (Highwood and Hoskins 1998).

The histograms for regimes with oceanic deep convection (Figs. 5c and 6c) also show that, while the deepest clouds are most prevalent in the early morning, middle- and low-level clouds appear most commonly during the afternoon and evening. This result is consistent with the characteristics of the diurnal cycle in mesoscale and submesoscale convective events reported by Rickenbach (1996) and Sui et al. (1997) based on TOGA COARE measurements. Rickenbach (1996) showed that submesoscale clouds typically extend only to the midtroposphere, near the freezing-level inversion (Johnson et al. 1999), and have their maximum amounts during afternoon and evening, much more typical of land-based convection. This is in contrast to the larger, mesoscale convective systems whose cloud tops often reach the upper troposphere. These systems display an early morning maximum in precipitation, consistent with the behavior of the cold clouds, as identified by the CLAUS precipitation algorithm and seen in the phase of diurnal harmonic (Figs. 3c and 3d). Similarly, Sui et al. (1997) describe the diurnal cycle in convection as one in which warm cumuli occur preferentially in the morning, convective showers in the afternoon, and organized convection, with heavy precipitation, at night. They note, in agreement with other studies, that the afternoon convective showers are most evident in undisturbed conditions, typical of the surpressed phase of the Madden–Julian oscillation.

5. Example of the use of CLAUS data to evaluate the simulated diurnal cycle

As noted in the introduction, the ability of a GCM to simulate correctly the phase and amplitude of the response of the land–ocean–atmosphere system to the diurnal cycle of solar radiation should be an important test of physical parameterization schemes. Here we show an example of the application of the CLAUS data to the evaluation of the diurnal cycle simulated by the climate, atmosphere-only version (HadAM3) of the Met. Office Unified Model (UM). To provide similar statistics on the diurnal cycle, the UM was integrated for a year with observed SSTs for 1991–92; 3-hourly diagnostics of OLR and precipitation were archived. Consequently the sample size from the model is rather limited, but future studies will focus on examining the diurnal cycle in the model in much more detail.

A full description of the model and its basic climate can be found in Pope et al. (2000). It contains a comprehensive suite of physical parametrizations, including state-of-the-art radiative transfer (Edwards and Slingo 1996), a fully interactive soil and vegetation land surface scheme (Cox et al. 1999), and a mass-flux convection scheme that is closed on buoyancy and includes convective momentum transport (Gregory et al. 1997). As described by Pope et al. (2000), this version of the UM provides a reasonable simulation of the tropical precipitation and circulation, although it still tends to underestimate the rainfall over the Maritime Continent and to overestimate the rainfall over the western Indian Ocean. These deficiencies are common to earlier versions of the UM and appear to be associated with the representation of the complex land–ocean system that exists around the Indonesian islands. In this study, the horizontal resolution of the model is 3.75° longitude by 2.5° latitude, its typical climate resolution. Versions of the model with 30 (L30) and 19 vertical levels have been evaluated. Since the results were found to be insensitive to vertical resolution, only those from the L30 version will be presented here.

The previous section has described the observed behavior of the diurnal cycle in radiation and convection in the CLAUS data. In this section, similar diagnostics will be presented based on the OLR and precipitation fields generated by the UM. To allow direct comparison with the CLAUS results, the model's OLR has been converted to an equivalent brightness temperature using Eqs. (1) and (2). When considering the model results, it is important to note that, whereas precipitation and T_b are uniquely related in the analysis of the CLAUS data through the use of Eq. (3), the same does not necessarily apply in the model. Variations in OLR, and hence equivalent T_b, will depend on how well the model's cloud scheme relates to the convection scheme.

The amplitudes of the diurnal harmonic in the simulated equivalent T_b and precipitation for DJF and JJA are shown in Fig. 7. In comparison with the results from

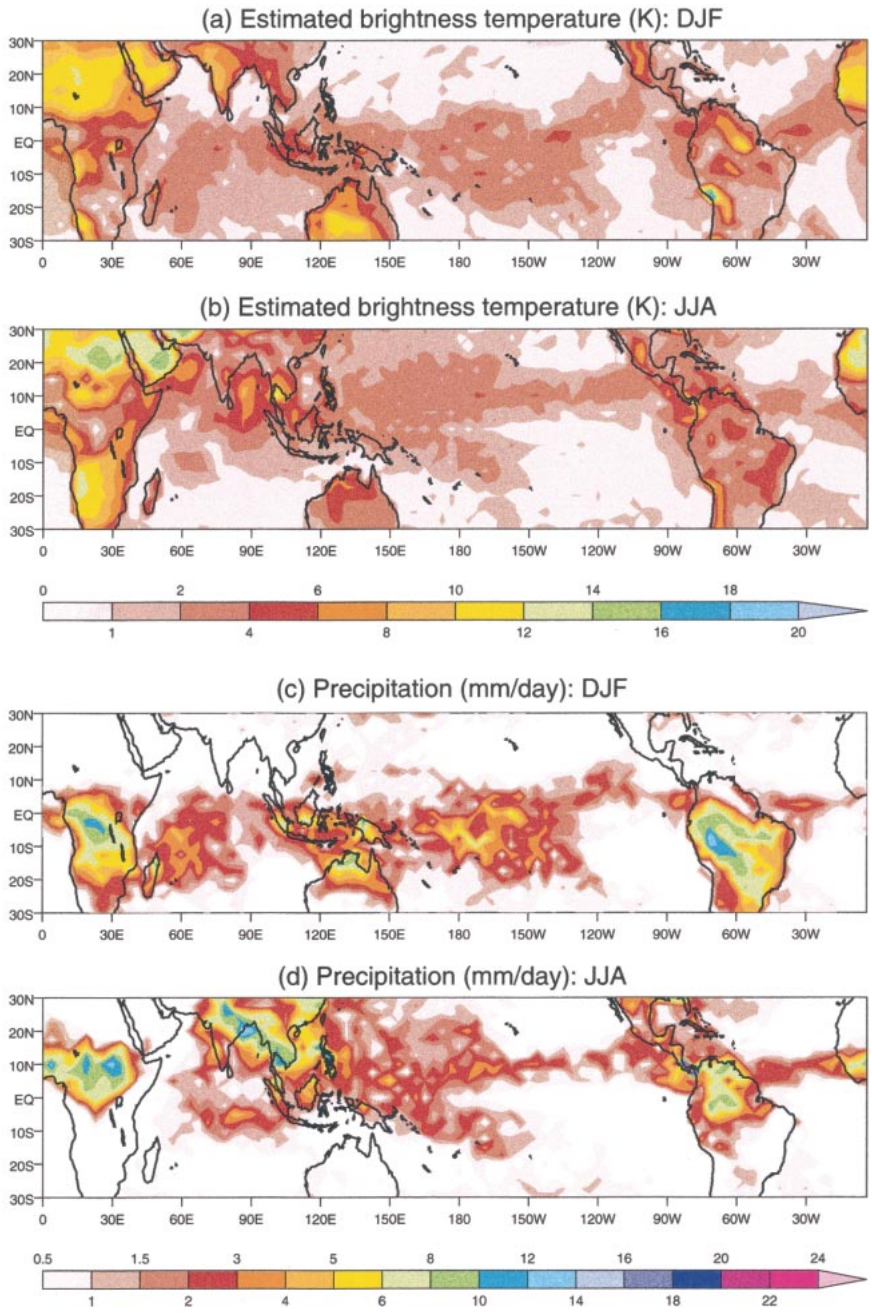

FIG. 7. Seasonal means amplitude of the diurnal harmonic of estimated brightness temperature (K) and precipitation (mm day^{-1}) from the L30 version of the Met. Office Unified Model for DJF and JJA.

CLAUS (Fig. 2), the model has successfully simulated many aspects of the amplitude of the diurnal harmonic. The spatial patterns are slightly different, which may be associated partly with systematic errors in the model's basic climate (Pope et al. 2000) and partly with the limited sample size. The amplitudes of the diurnal harmonic in equivalent T_b are generally well captured over the clear sky land areas of North Africa, but are underestimated for Australia, particularly during southern winter. The diurnal amplitude in precipitation over continental convective regions, such as South Africa in DJF and central Africa in JJA, is generally well captured. Obvious discrepancies are over the islands of the Maritime Continent in DJF and over the Indian monsoon region in JJA. The model has failed to capture the pronounced diurnal cycle over northern India, but has simulated rather large amplitudes in equivalent T_b over the Arabian Sea and Bay of Bengal (Fig. 7b), which are

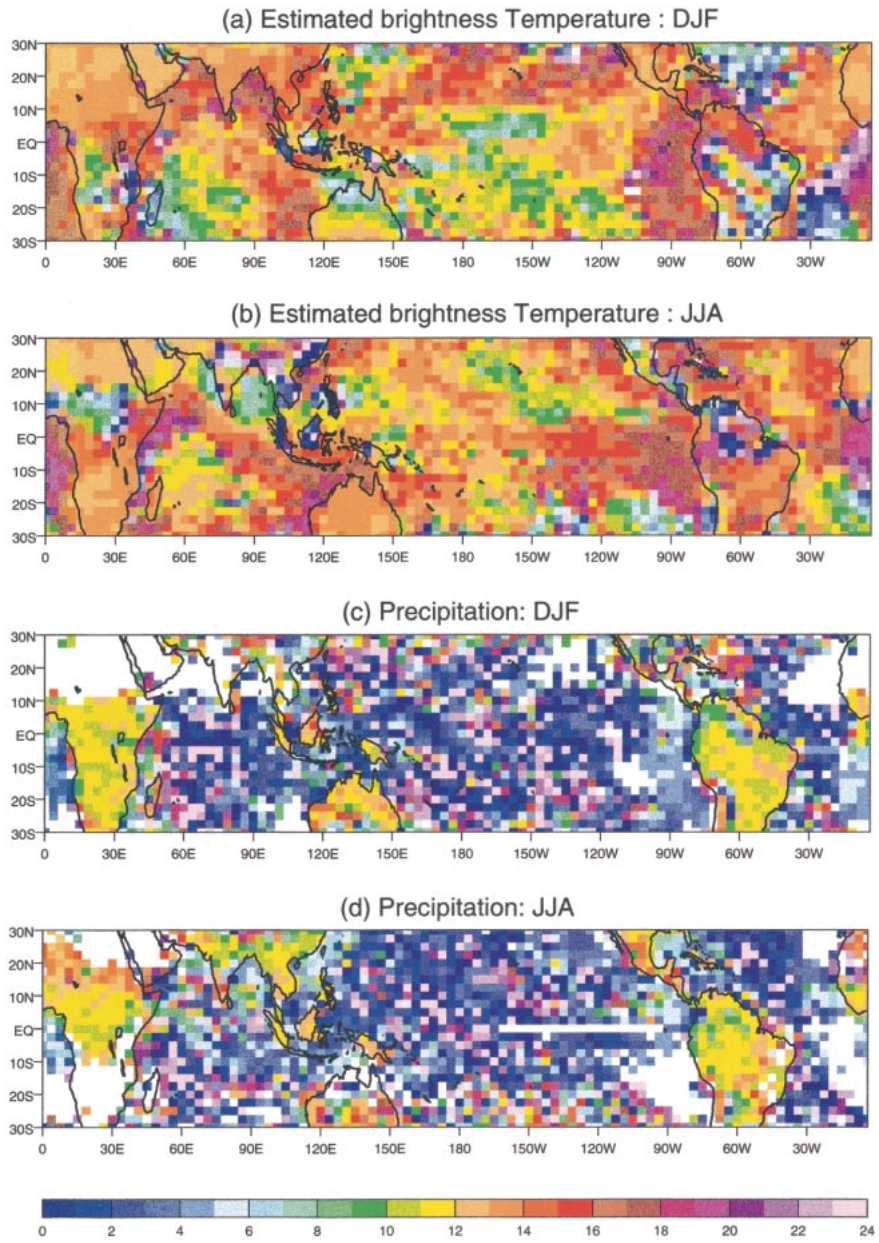

FIG. 8. Seasonal mean phase of the diurnal harmonic of estimated brightness temperature and precipitation from the L30 version of the Met. Office Unified Model for DJF and JJA. The local time of maximum is given.

not collocated with those in precipitation (Fig. 7d), nor seen in the CLAUS results (Fig. 2). Over the open oceans, the model appears to have slightly overestimated the amplitude of the diurnal harmonic in equivalent T_b but underestimated it in precipitation, although the limitations of the CLAUS results should be noted, since they rely on simple algorithms to relate T_b to precipitation.

The phase of the diurnal harmonic of equivalent T_b and precipitation from the UM is shown in Fig. 8. In comparison with the CLAUS results (Fig. 3), it is evident that the UM poorly simulates the phase of the diurnal harmonic of the equivalent T_b and precipitation in the Tropics for both seasons. The most marked discrepancy occurs for convective regimes. According to Fig. 8, for land convective regimes, the diurnal maximum in the simulated precipitation occurs before noon, instead of in the late afternoon and evening as indicated in the CLAUS data (Fig. 3). The model is more successful at simulating the time of maximum equivalent T_b, which generally in the midmorning is in agreement with the CLAUS results. A notable exception is over

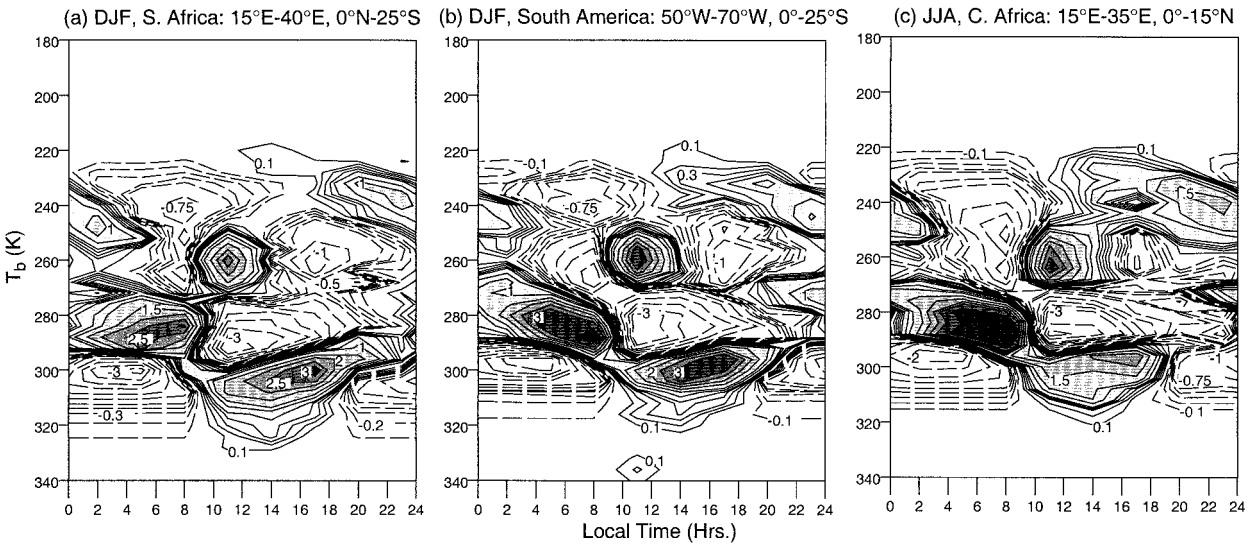

FIG. 9. Seasonal mean evolution histograms of the diurnal variation in estimated brightness temperature from the Unified Model for land convective regimes. The contours represent percentage departures from the daily mean histogram of estimated brightness temperature.

Brazil in JJA where the model gives a near-midnight maximum in equivalent T_b that is quite different from any of the other land convective regions.

The UM also advances the timing of the simulated diurnal maximum in oceanic precipitation, which appears around midnight, in contrast to the estimates from the CLAUS data where the maximum convection occurs typically about 6 h later in the early morning. Even allowing for the likelihood that the phase results for precipitation, estimated from the CLAUS data, may be later than reality by up to 3 h (e.g., Janowiak et al. 1994), it is clear that the UM produces a diurnal maximum in precipitation that is too early in the day. There is also a lesser discrepancy over land clear sky regions, where the model gives a maximum in equivalent T_b coincident with the peak in solar heating, 1–2 h earlier than that observed in the CLAUS data.

Using 3-hourly diagnostics of equivalent T_b from the UM, evolution histograms typical of continental and oceanic convection have been constructed in a similar manner to those based on T_b from the CLAUS dataset. Although the histograms are not nearly as well sampled as in the CLAUS results (coarser grid, 1 yr only), the results nevertheless reveal systematic errors in the model. Figure 9 shows three examples of the histograms for land convective regimes that are characterised by a precipitation maximum near noon in Fig. 8. All show a very similar behavior that does not compare well with the CLAUS results shown in Figs. 5 and 6. As soon as the land surface begins to warm up in the morning, convection is initiated that reaches to the midtroposphere. Soon after, the convection extends to the upper troposphere with the lowest values of equivalent T_b typically occurring in the midafternoon, compared to the evening in the CLAUS data.

For oceanic convection (Fig. 10), the histograms are quite noisy since the diurnal cycle is quite weak and therefore difficult to sample. Nevertheless, the results given in Fig. 10, for two oceanic convective regimes, again show similar characteristics that support the phase results shown in Fig. 8. The deepest convection tends to occur in the late afternoon in the model compared with the early morning in the CLAUS data (Figs. 5 and 6).

6. Discussion and conclusions

The CLAUS multiyear, high spatial and temporal resolution global dataset of brightness temperature has provided a unique opportunity to carry out a systematic investigation of the diurnal variation in convection and radiation over the whole Tropics. The characteristics of the diurnal cycle described by the CLAUS data agree with previous observational studies cited in the introduction. Whereas those studies were mostly for limited regions and short time samples, the CLAUS results have demonstrated the universality of the characteristics of the diurnal cycle for land versus ocean, clear sky versus convective regimes. They have also shown some interesting regional variations indicative of the effects of complex land–sea and mountain–valley breezes, as well as the life cycle of mesoscale convective systems.

A striking result from the analysis of the CLAUS data has been the extent to which the strong diurnal signal over land is spread out over the adjacent oceans, probably through gravity waves of varying depths. These coherent signals can be seen for several hundred kilometers and in some instances, such as over the Bay of Bengal, can lead to substantial diurnal variations in convection and precipitation. Over the complex system of islands that make up the Maritime Continent, these coherent signals in the diurnal cycle represent important

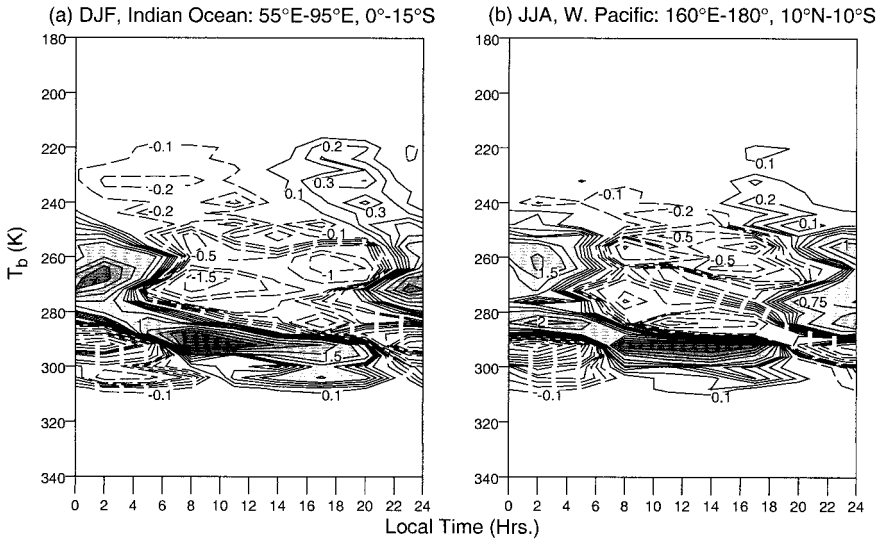

FIG. 10. As in Fig. 9 but for oceanic convective regions.

land–sea-breeze effects that may play a crucial role in the heat and moisture budget of this key region for the tropical and global circulation.

The results have shown that the diurnal cycle for various tropical regions with different characteristics is substantially different. The largest amplitudes of the diurnal harmonic of T_b occur over the clear sky continents with a maximum in T_b in the early afternoon, 1–2 h after the maximum in solar heating. For convective regimes, the diurnal amplitude is larger and more spatially consistent over the continents than over the oceans. For both DJF and JJA, oceanic deep convection tends to reach its maximum in the early morning, while continental convection typically peaks in the evening.

The phase of the diurnal harmonic suggests that the mechanisms for the observed diurnal variation in convection over land and ocean are very different. The diurnal cycle of convection over land is basically a low-level themodynamical response to the radiative heating cycle. During the day, solar heating over land surface increases the lower-tropospheric temperature (and moisture) and hence instability, leading to development of convection, the resulting convective precipitation maximum tending to occur in the evening. In contrast, radiative cooling of the land surface at night enhances the stability, suppressing convection and leading to a minimum in the early morning. This idealized view of the diurnal cycle over land is modified by local orography and by the initiation, propagation, and decay of mesoscale convective systems, such as squall lines.

For deep oceanic convection, which typically peaks in the early morning, the situation is much more complicated, and there may be several mechanisms responsible for the behavior of the diurnal cycle. The first involves a direct radiation–convection interaction (Randall et al. 1991). At night, infrared cooling at the cloud top is greater than at cloud base resulting in destablization of the upper troposphere, leading to cloud development with a maximum occurring in the early morning; during the day, warming at cloud top due to solar absorption increases the stability and therefore restricts convective activity.

The second possible mechanism involves the cloud versus cloud-free radiation difference in the horizontal (Gray and Jacobson 1977). The radiative cooling of the cirrostratus at upper-tropospheric levels is greater than the radiative cooling in the surrounding less cloudy or clear sky regions, whereas during the day the situation is reversed. This day–night differential heating cycle results in a daily variation in the horizontal divergence field that may give rise to a diurnal variation in convective activity. Recently, Liu and Moncrieff (1998) used an idealized two-dimensional cloud resolving numerical model to simulate the diurnal variation of tropical oceanic deep convection. The model gave a predawn maximum and late afternoon minimum in convection intensity for highly organized as well as less organized convection. Liu and Moncrieff (1998) concluded that this diurnal variation was primarily controlled by the direct radiation–convection interaction; the cloud versus cloud-free radiation difference was of secondary importance.

However, Chen and Houze (1997) have suggested that the mechanism for the diurnal cycle of tropical oceanic deep convection involves a rather complex surface–cloud–radiation interaction, not just a cloud–radiation interaction. They argue that the cloud–radiation interaction mechanism can only partially explain the diurnal cycle of the tropical oceanic deep convection. It does not explain why the large-scale convective systems, which contribute most to the observed night-to-dawn maximum in cold cloud cover and precipitation, usually start preferentially in the afternoon, a time that is unfavorable in terms of atmospheric radiative processes.

Chen and Houze (1997) point out that surface and near-surface thermal variables relevant to convective variability (i.e., skin sea surface temperature and surface air temperature) consistently reach their maximum in the afternoon and that the phasing of the diurnal cycle in these variables is favorable to the afternoon initiation of convective systems. Some of these convective systems, under optimal environmental conditions, continue to grow and reach their mature stage some time later during the night and early morning.

Chen and Houze (1997) also suggest that besides the nature of the underlying surface, an additional factor affecting the diurnal cycle in tropical deep convection is the life cycle of cloud systems themselves. Because the life cycle of large convective systems can take up to a day, they leave the boundary layer filled with air of lower moist-static energy and a cloud canopy that partially shades the ocean surface from the sunlight the following day. Since the surface conditions are unfavorable for another round of widespread convection, the next day's convection tends to occur in neighboring regions unaffected by the previous convective systems. They call this spatial variability of the diurnal cycle of the large convective systems ''diurnal dancing,'' which may trigger and phase lock with westward propagating inertio–gravity waves of similar 2-day period.

The example of the use of the CLAUS data in the evaluation of the Met. Office Unified Model has demonstrated that the model has considerable difficulty in capturing the observed phase of the diurnal cycle in convection. This has been noted also in numerical weather prediction applications of the model (Ringer 1998). This may suggest some fundamental difficulties in the model's physical parameterizations. Possible candidates to be considered are the land surface scheme and its response to solar heating, the planetary boundary layer and its communication with the surface and the free troposphere, and the convection scheme and its response to near-surface buoyancy.

However, some of the problems in the phase of the diurnal cycle in the UM may be related to the technical implementation of the radiation scheme. Comprehensive radiation calculations are computationally demanding and, in common with many other atmospheric GCMs (see Phillips 1994), the UM only calls the full radiation scheme every 3 h. At intermediate time steps, a simple radiation calculation is made, based on the shortwave and longwave fluxes from the full radiation calculation. To allow for the diurnal variation in the incoming solar radiation, the shortwave fluxes are adjusted by the solar zenith angle on the intermediate time steps but the clouds and the temperatures essentially remain fixed between the 3-hourly calls to the full radiation calculation. This may have serious implications for the diurnal cycle, particularly over land where the surface temperature should respond rapidly to the diurnal cycle in solar forcing. Also the use of fixed clouds essentially means that the cloud field can be on average 1.5 h out of phase with the solar forcing.

To investigate how much of the discrepancy between the observed and simulated diurnal cycles might be explained by the technical implementation of the radiation code, a year's integration was performed in which the full radiation calculation was made every time step and, hence, was as accurate as possible. In terms of both the amplitude and the phase of the diurnal harmonic, the results were quite similar, except over clear sky land (desert) regions where the time of maximum inferred brightness temperature was 1–2 h later, in better agreement with the CLAUS data. This is well demonstrated in Figs. 11a and 11b. With the standard 3-hourly calls to the full radiation calculation (Fig. 11a), the model has produced its warmest land surface temperatures before noon, due to the imbalance between the solar heating and the longwave cooling. When the radiation is calculated accurately (Fig. 11b), the shape of the evolution histogram is much closer to the observed behavior (cf. Fig. 7a), with the warmest temperatures occurring in the early afternoon. As is also evident in Figs. 11a and 11b, the amplitude of the diurnal cycle is slightly reduced with the full radiation calculation.

For land convective regimes, the implementation of an accurate radiation calculation has had little impact on the model's major systematic error in the phase of diurnal cycle in precipitation. The rainfall still occurs preferentially before noon. However, the evolution histogram shown in Fig. 11c does suggest that the detailed behavior of the diurnal cycle is affected by the accuracy of the radiation calculation. There is now a more gradual evolution of the cloud field and the tendency for large amounts of middle-level cloudiness to appear suddenly just before noon has been removed (cf. Fig. 9). Nevertheless, the fact that the model's rainfall still occurs preferentially before noon suggests that there are fundamental shortcomings in the response of the surface, boundary layer, and convective parametrizations to the diurnal cycle in shortwave heating.

The implementation of an accurate radiation calculation has also had little impact on the simulated diurnal cycle in oceanic convection. Returning to the results of Chen and Houze (1997) discussed above, it is clear that the Unified Model (and indeed other atmospheric GCMs) may lack potential key ingredients to produce the correct diurnal cycle in convection over the oceans. First, the model uses a fixed SST and so there is no allowance for diurnal variations in skin sea surface temperature such as was observed during TOGA COARE (e.g., Weller and Anderson 1996). These variations in skin temperature can be large ($>$1 K), particularly in light wind, undisturbed conditions (e.g., Webster et al. 1996), and appear to be important for triggering convection. Second, the model's convective parameterization involves an instantaneous adjustment and is therefore unlikely to represent the gradual growth of a convective system as described by Chen and Houze (1997).

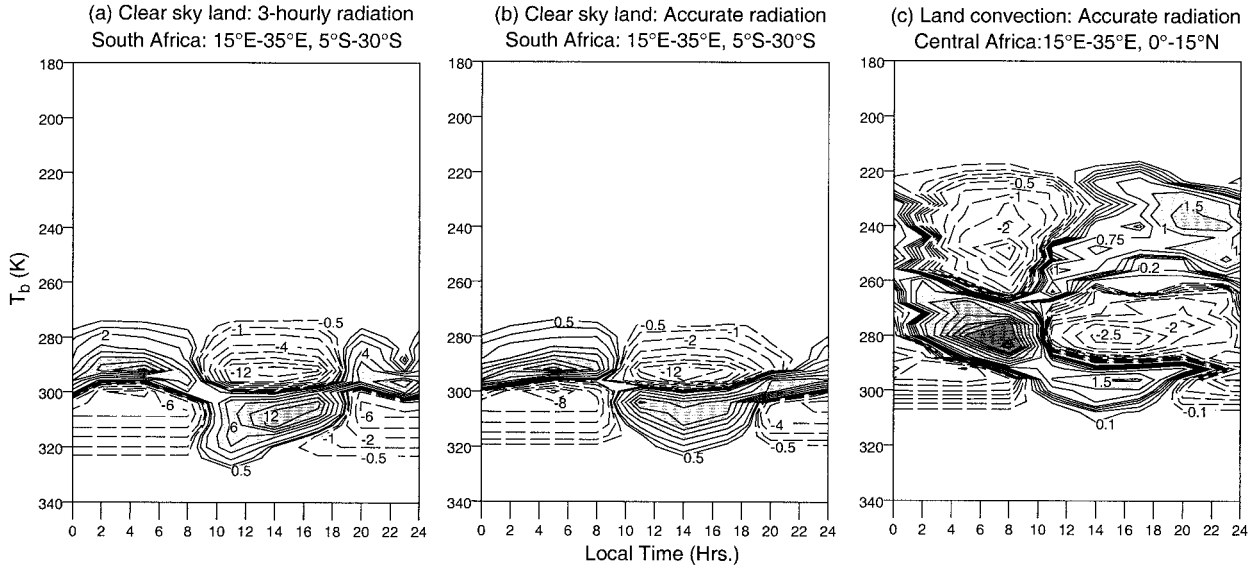

FIG. 11. Evolution histograms showing the effect of performing a full radiation calculation every model time step. (a) and (b) Evolution of the estimated brightness temperature for a land clear sky regime (South Africa in JJA) for 3-hourly and accurate radiation calculations, respectively. (c) Evolution of the estimated brightness temperature for a land convective regime (central Africa in JJA) from the accurate radiation calculation. It can be compared with Fig. 9c.

It is possible that the convective parameterization may need to carry a history of the life cycle of the cloud systems, suggesting major changes in our current approach to convective parametrization.

This paper has shown the considerable potential that diurnal cycle diagnostics possess for demonstrating model deficiencies. The results support the argument that as a basic, forced mode of the climate system, the ability of general circulation models to represent the diurnal cycle should be a key test of the correctness of any model. Future research will involve a more-detailed analysis of the diurnal cycle in the Unified Model, as well as experimentation with a hierarchy of models, including a cloud resolving model, to investigate the coupling between the surface, boundary layer, and free troposphere on diurnal timescales.

Acknowledgments. Gui-Ying Yang was supported by the EC project, Cloud Archive User Service (ENV4-CT96-0356). Julia Slingo acknowledges the support of the NERC U.K. Universities' Global Atmospheric Modelling Programme. Richard Neale is thanked for providing results from the additional integration with the full radiation calculation. Helpful comments by Dr. Steven Sherwood on the original version are gratefully acknowledged.

REFERENCES

Albright, M. D., D. R. Mock, E. E. Recker, and R. J. Reed, 1981: A diagnostic study of the diurnal rainfall variation in the GATE B-scale area. *J. Atmos. Sci.,* **38,** 1429–1445.

——, E. E. Recker, R. J. Reed, and R. Dang, 1985: The diurnal variation of deep convection and inferred precipitation in the central tropical Pacific during January–February 1979. *Mon. Wea. Rev.,* **113,** 1663–1680.

Augustine, J. A., 1984: The diurnal variation of large-scale inferred rainfall over the tropical Pacific Ocean during August 1979. *Mon. Wea. Rev.,* **112,** 1745–1751.

Bergman, J. W., and M. L. Salby, 1996: Diurnal variations of cloud cover and their relationship to climatological conditions. *J. Climate,* **9,** 2802–2820.

Betts, A. K., and J. H. Ball, 1995: The FIFE surface diurnal cycle climate. *J. Geophys. Res.,* **100,** 25 679–25 693.

Brest, C. L., W. B. Rossow, and M. Roiter, 1997: Update of radiance calibrations for ISCCP. *J. Atmos. Oceanic Technol.,* **14,** 1091–1109.

Chang, A. T. C., L. S. Chiu, and G. Yang, 1995: Diurnal cycle of oceanic precipitation from SSM/I data. *Mon. Wea. Rev.,* **123,** 3371–3380.

Chen, S. S., and R. A. Houze, 1997: Diurnal variation and life-cycle of deep convective systems over the tropical Pacific warm pool. *Quart. J. Roy. Meteor. Soc.,* **123,** 357–388.

Cox, P. M., R. A. Betts, C. B. Bunton, R. L. H. Essery, P. R. Rowntree, and J. Smith, 1999: The impact of new land surface physics on the GCM simulation of climate and climate sensitivity. *Climate Dyn.,* **15,** 183–203.

Edwards, J. M., and A. Slingo, 1996: Studies with a flexible new radiation code. I: Choosing a configuration for a large-scale model. *Quart. J. Roy. Meteor. Soc.,* **122,** 689–719.

Fu, R., A. Del Genio, and W. B. Rossow, 1990: Behavior of deep convective clouds in the tropical Pacific from ISCCP radiances. *J. Climate,* **3,** 1129–1152

Garreaud, R. D., and J. M. Wallace, 1997: The diurnal march of convective cloudiness over the Americas. *Mon. Wea. Rev.,* **125,** 3157–3171.

Goodman, B., W. P. Menzel, E. C. Cutrim, and D. W. Martin, 1993: A non-linear algorithm for estimating 3-hourly rain rates over Amazonia from GOES/VISSR observations. *Remote Sens. Rev.,* **10,** 169–177.

Gray, W. M., and R. W. Jacobson, 1977: Diurnal variation of deep cumulus convection. *Mon. Wea. Rev.,* **105,** 1171–1188.

Gregory, D., R. Kershaw, and P. M. Inness, 1997: Parametrization of momentum transport by convection. II: Tests in single-column

and general circulation models. *Quart. J. Roy. Meteor. Soc.,* **123,** 1153–1183.

Harrison, E. F., P. Minnis, B. R. Barkstrom, V. Ramanathan, R. D. Cess, and G. G. Gibson, 1990: Seasonal variation of cloud radiative forcing derived from the Earth Radiation Budget Experiment. *J. Geophys. Res.,* **95,** 18 687–18 703.

Hendon, H. H., and K. Woodberry, 1993: The diurnal cycle of tropical convection. *J. Geophys. Res.,* **98,** 16 523–16 637.

Highwood, E. J., and B. J. Hoskins, 1998: The tropical tropopause. *Quart. J. Roy. Meteor. Soc.,* **124,** 1579–1604.

Hignett, P., 1991: Observations of the diurnal variation in a cloud-capped marine boundary layer. *J. Atmos. Sci.,* **48,** 1474–1482.

Hodges, K. I., and C. D. Thorncroft, 1997: Distribution and statistics of African mesoscale convective weather systems based on the ISCCP Meteosat imagery. *Mon. Wea. Rev.,* **125,** 2821–2837.

——, D. W. Chappell, G. J. Robinson, and G. Yang, 2000: An improved algorithm for generating global window brightness temperatures from multiple satellite infrared imagery. *J. Atmos. Oceanic Technol.,* **17,** 1296–1312.

Houze, R. A., S. G. Geotis, F. D. Marks, and A. K. West, 1981: Winter monsoon convection in the vicinity of north Borneo. Part I: Structure and time variation of clouds and precipitation. *Mon. Wea. Rev.,* **109,** 1595–1614.

Janowiak, J., P. A. Arkin, and M. Morrissey, 1994: An examination of the diurnal cycle in oceanic tropical rainfall using satellite and in situ data. *Mon. Wea. Rev.,* **122,** 2296–2311.

Johnson, R. H., and D. C. Kriete, 1982: Thermodynamic and circulation characteristics of winter monsoon tropical mesoscale convection. *Mon. Wea. Rev.,* **110,** 1898–1911.

——, T. M. Rickenbach, S. A. Rutledge, P. E. Ciesielski, and W. H. Schubert, 1999: Trimodal characteristics of tropical convection. *J. Climate,* **12,** 2397–2418.

Kousky, V. E., 1980: Diurnal rainfall variation in northeast Brazil. *Mon. Wea. Rev.,* **108,** 488–498.

Liu, C., and M. W. Moncrieff, 1998: A numerical study of the diurnal cycle of tropical oceanic convection. *J. Atmos. Sci.,* **55,** 2329–2344.

Mapes, B. E., and R. A. Houze, 1993: Cloud clusters and superclusters over the oceanic warm pool. *Mon. Wea. Rev.,* **121,** 1398–1415.

McGarry, M. M., and R. J. Reed, 1978: Diurnal variations in convective activity and precipitation during phases II and III of GATE. *Mon. Wea. Rev.,* **106,** 101–113.

Morcrette, J.-J., 1991: Evaluation of model-generated cloudiness: Satellite-observed and model-generated diurnal variability of brightness temperature. *Mon. Wea. Rev.,* **119,** 1205–1224.

Ohring, G., and A. Gruber, 1984: Satellite determination of the relationship between total longwave radiation flux and infrared window radiance. *J. Climate Appl. Meteor.,* **23,** 416–425.

Phillips, T. J., 1994: A summary documentation of the AMIP models. PCMDI Rep. 18, 343 pp. [Available from Program for Climate Model Diagnosis and Intercomparison, Lawrence Livermore National Laboratory, Livermore, CA 94550.]

Pope, V. D., M. L. Gallani, P. R. Rowntree, and R. A. Stratton, 2000: The impact of new physical parameterizations in the Hadley Centre climate model—HadAM3. *Climate Dyn.,* **16,** 123–146.

Randall, D. A., Harshvardhan, and D. A. Dazlich, 1991: Diurnal variability of the hydrologic cycle in a general circulation model. *J. Atmos. Sci.,* **48,** 40–62.

Richards, F., and P. A. Arkin, 1981: On the relationship between satellite observed cloud cover and precipitation. *Mon. Wea. Rev.,* **109,** 1081–1093.

Rickenbach, T. M., 1996: Convection in TOGA COARE: Horizontal scale, morphology, and rainfall production. Ph.D. dissertation, Department of Atmospheric Science Paper 630, Colorado State University, Fort Collins, CO.

Ringer, M., 1998: Tropical convective rainfall in the global UM: Initial comparisons with estimates derived from Meteosat infrared imagery. Forecasting Research Tech. Rep. 239, The Met. Office, Bracknell, United Kingdom, 33 pp.

Rossow, W. B., A. Walker, and M. Roiter, 1997: International Satellite Cloud Climatology Project (ISCCP): Description of reduced resolution radiance data. WMO/TD-No. 58.

Rowell, D. P., and J. R. Milford, 1993: On the generation of African squall lines. *J. Climate,* **6,** 1181–1193.

Salby, M. L., H. H. Hendon, K. Woodberry, and K. Tanaka, 1991: Analysis of global cloud imagery from multiple satellites. *Bull. Amer. Meteor. Soc.,* **72,** 467–480.

Shin, K.-S., G. R. North, Y.-S. Ahn, and P. A. Arkin, 1990: Time scales and variability of area-averaged tropical oceanic rainfall. *Mon. Wea. Rev.,* **118,** 1507–1516.

Slingo, J. M., K. R. Sperber, J.-J. Morcrette, and G. L. Potter, 1992: Analysis of the temporal behavior of convection in the tropics of the European Centre for Medium-Range Weather Forecasts model. *J. Geophys. Res.,* **97,** 18 119–18 135.

——, and Coauthors, 1994: Mean climate and transience in the tropics of the UGAMP GCM: Sensitivity to convective parameterization. *Quart. J. Roy. Meteor. Soc.,* **120,** 881–922.

Smith, W. S., and C.-Y. J. Kao, 1996: Numerical simulations of the marine stratocumulus-topped boundary layer and its diurnal variation. *Mon. Wea. Rev.,* **124,** 1803–1816.

Sui, C.-H., K.-M. Lau, Y. N. Takayabu, and D. A. Short, 1997: Diurnal variations in tropical oceanic cumulus convection during TOGA COARE. *J. Atmos. Sci.,* **54,** 639–655.

Wallace, J. M., 1975: Diurnal variations in precipitation and thunderstorm frequency over the conterminous United States. *Mon. Wea. Rev.,* **103,** 406–419.

Webster, P. J., C. A. Clayson, and J. A. Curry, 1996: Clouds, radiation and the diurnal cycle of sea surface temperature in the tropical western Pacific Ocean. *J. Climate,* **9,** 1712–1730.

Weller, R. A., and S. P. Anderson, 1996: Surface meteorology and air–sea fluxes in the western equatorial Pacific warm pool during the TOGA Coupled Ocean–Atmosphere Response Experiment. *J. Climate,* **9,** 1959–1990.

Williams, M., and R. A. Houze, 1987: Satellite-observed characteristics of winter monsoon cloud clusters. *Mon. Wea. Rev.,* **115,** 505–519.

Xie, P., and P. A. Arkin, 1996: Analyses of global monthly precipitation using gauge observations, satellite estimate, and numerical model precipitation. *J. Climate,* **9,** 840–858